

First Principles Investigation of $Al_2O_3/\beta-Ga_2O_3$ Interface Structures

Junsung Park and Sung-Min Hong
 School of Electrical Engineering and Computer Science
 Gwangju Institute of Science and Technology
 Gwangju 61005, Republic of Korea
 smhong@gist.ac.kr

Abstract—The $\beta-Ga_2O_3$ (beta-gallium oxide) is one of promising candidate materials for the future power and RF devices. Since the high-quality gate dielectric layer is mandatory for developing the Ga_2O_3 based MOSFET, theoretical investigation on the properties of $Al_2O_3/\beta-Ga_2O_3$ interface is required. We have generated atomistic $Al_2O_3/\beta-Ga_2O_3$ interface models, which are consistent with experimental results. By the density functional theory (DFT)-based electronic structure calculation, it is confirmed that the generated interface structures are physically stable. The band offset levels are applicable to the MOS structure for device application. It is expected that the atomistic interface structures generated in this work can be used for further first principles investigation on the $Al_2O_3/\beta-Ga_2O_3$ interface.

Index Terms—Density functional theory, interface structure, $\beta-Ga_2O_3$, Al_2O_3

I. INTRODUCTION

The $\beta-Ga_2O_3$ is one of the most promising candidate materials for future power electronic devices [1]–[3]. $\beta-Ga_2O_3$ based devices are expected to exhibit better performance than state-of-arts 4H-SiC and GaN-based power devices because of its wide bandgap ($E_g = 4.4 - 4.6\text{eV}$), high breakdown electric field (8MV/cm), and high-productivity. Many gallium oxide based devices have been reported recent years, such as Schottkey diodes, MESFETs, and MOSFETs [1]–[3]. For the device fabrication, (010) and $(\bar{2}01)$ plane oriented crystalline substrates are commonly used.

The quality of an interface between a gate dielectric and $\beta-Ga_2O_3$ is a key performance factor of the electronic devices. Usually, chemical-vapor deposited or atomic-layer deposited (ALD) *amorphous- Al_2O_3* layers are mainly used as a gate dielectric. Especially, recently reported papers suggest crystalline dielectric layer growth [4], [5]. Few nano-meters $\gamma-Al_2O_3$ phase layer can grow on the (010) $\beta-Ga_2O_3$ substrate by the ALD process. Since it is very important to find the band offsets at an interface structure, for the device design, many experiments have been performed. However, depending on the process conditions, experimental results show large differences even in the same dielectric material.

In this study, we perform the structure generation and structure minimization process to find the interface of the lowest total energy of the system. We obtain the band offset by electronic structure calculation. Both *amorphous- Al_2O_3* (*am- Al_2O_3*) and crystalline $\gamma-Al_2O_3$ heterojunction interfaces are studied. In Sec. II, the overall calculation procedure the

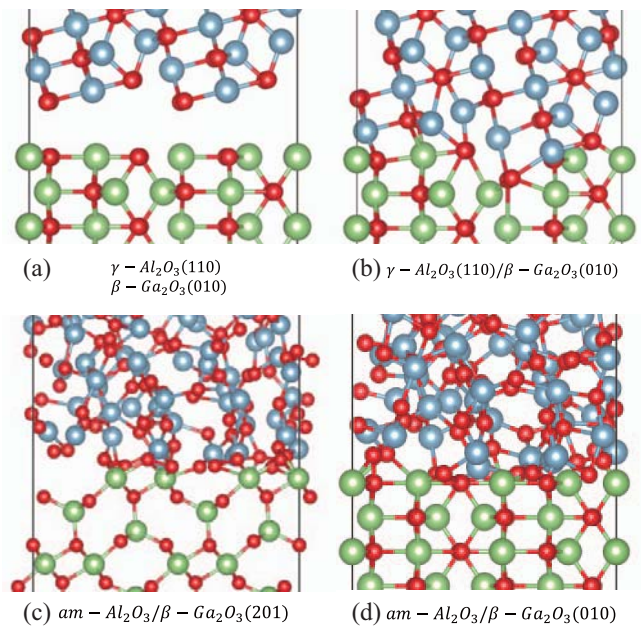


Figure 1 : Atomistic models representing Al_2O_3/Ga_2O_3 interfaces. (a) The crystalline planes of both $\gamma-Al_2O_3(110)$ and $\beta-Ga_2O_3$. (b) The optimized $\gamma-Al_2O_3(110)/\beta-Ga_2O_3$ interface. The structure is obtained through the removal of the atoms at the overlapping positions, the location reorientation, and the DFT-MD optimization process. (c) and (d) are optimized *am- Al_2O_3* / $\beta-Ga_2O_3$ interfaces. The optimization process for obtaining each structure is the same as (b).

generation process of interface models are discussed. In Sec. III, the analysis based on the DFT calculation of the interface models is presented. Finally, in Sec. IV, the conclusion is drawn.

II. CALCULATION METHODS

All of the electronic structure calculations are performed by a DFT simulation package, Vienna ab initio simulation package (VASP) [6]. The Perdew-Burke-Ernzerhof (PBE) exchange-correlation potential is used for geometry optimization [7]. Structural minimization has been performed until all the atomic forces are less than $0.01\text{eV}/\text{\AA}$. One of the critical problems of the conventional DFT calculation is the bandgap

Method	Material	Bandgap(eV)
Experiments	γ -Al ₂ O ₃	8.7
	β -Ga ₂ O ₃	4.65
GGA-PBE	γ -Al ₂ O ₃	4.84
	β -Ga ₂ O ₃	2.44
MetaGGA (non-regular TB-mBJ)	γ -Al ₂ O ₃	8.1
	β -Ga ₂ O ₃	4.62

Table 1 : Comparison of bandgap results of each material. Common GGA-PBE functional underestimated the bandgap of materials used in this paper. (GGA, generalized gradient approximation)

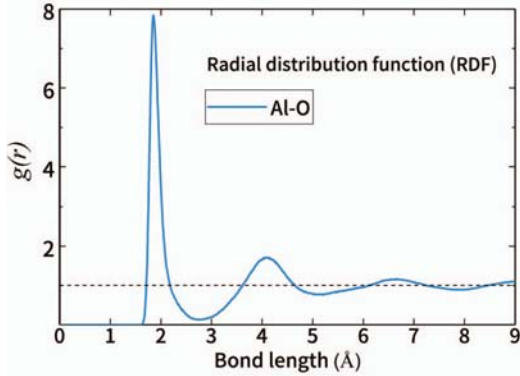


Figure 2 : Radial distribution results of MD-generated *amorphous*-Al₂O₃.

underestimation for many semiconductor materials [8], [9]. For the calibration of the bandgap, we use a Tran-Blaha's modified Becke-Johnson (TB-mBJ) Meta-GGA functional which is well matched with hybrid functionals and GW methods [8], [10], [11]. Especially, the non-regular TB-mBJ method has been used for accurate bandgap matching with experimental data [12], [13].

Table 1 shows the optimized bandgap values using the non-regular TB-mBJ functional. In the case of the conventional GGA-PBE functional, the bandgap is predicted to be relatively lower than the experimental value. In the case of the non-regular TB-mBJ method with optimized parameters for each material, electronic band structures are similar to the experimental result [13]. The non-regular TB-mBJ potential was proposed as,

$$V^{TB-mBJ}(r) = cV^{BR}(r) + (3c - 2)\frac{1}{\pi}\sqrt{\frac{5}{6}}\sqrt{\frac{t(r)}{\rho(r)}} \quad (1)$$

where $V^{BR}(r)$ is the Beck-Roussel(BR) exchange potential and $\rho(r) = \sum_i^N |\psi_i|^2$ is the electron density. Moreover, the Kohn-Sham (KS) kinetic energy density, $t(r)$, is given by

$$t(r) = \frac{1}{2} \sum_i^N \nabla \psi_i^*(r) \cdot \nabla \psi_i(r). \quad (2)$$

Method	Material (E_g)		c parameter optimization
	$\gamma - Al_2O_3$	$\beta - Ga_2O_3$	
TB-mBJ (c_{opt})	6.55 (1.37)	4.61 (1.404)	SC
Non-reg TB-mBJ (c_{adj})	8.23 (1.82)	4.76 (1.42)	Manual
Non-reg TB-mBJ (c_{atoms})	8.1 ($c_{Al} = 1.87$ $c_O = 1.42$)	4.62 ($c_{Ga} = 1.42$ $c_O = 1.42$)	Manual

Table 2 : Bandgap values obtained by using the TB-mBJ functional for $\gamma - Al_2O_3$ and $\beta - Ga_2O_3$ materials. The first row is the bandgap obtained using the conventional TB-mBJ method. c_{opt} is a self-consistently (SC) evaluated coupling parameter. The second and third are the results using the coupling parameter set for reproducing experimental gaps. c_{atoms} is a coupling parameter for each atom used in the interface calculation.

The coupling parameter c between the BR exchange potential and the electron density-related term is given by

$$c = \alpha + \beta \left(\frac{1}{V_{cell}} \int_{cell} \frac{|\nabla \rho(\mathbf{r}')|}{\rho(\mathbf{r}')} d\mathbf{r}' \right)^{\frac{1}{2}} \quad (3)$$

The coupling parameter c is obtained by the self-consistent (SC) process during the DFT calculation. (Usually, $\alpha = -0.012$ and $\beta = 1.023$ are used for the conventional TB-mBJ simulation). In many cases, the TB-mBJ functional can obtain bandgaps similar to the experimental values [8], [10]. However, as shown in Table 2, the calculated bandgap of $\gamma - Al_2O_3$ is still lower than the experimental result. The DFT calculated result is nearly 2eV lower than the experimental one. In this case, the coupling parameter c is adjusted to make the bandgap similar to the experimental value. This method is called non-regular TB-mBJ functional. An appropriate c value matching the experimental result is selected. In this study, we adopt the coupling parameter c as follows: $c_{Al} = 1.87$, $c_{Ga} = 1.42$, and $c_O = 1.42$. By using these values, the bandgap obtained by DFT calculation and and experimental gap agree very well (see Table 2).

An *am*-Al₂O₃ atomistic structure is generated from 2-step MD simulations. The first step is reactive force-field (ReaxFF) molecular dynamics (MD) simulation under the condition that the temperature decreases from 900K to 300K for 20 ps. The second step is structural minimization by the DFT-MD simulations [14]. In order to verify the generated amorphous model, we have calculated the radial distribution function (RDF) and neutron static scattering factor. The agreement with the experimental results is confirmed. The final structure is shown in Fig. 1 (b) and the RDF of generated *am*-Al₂O₃ model is shown in Fig. 2 [15].

III. CALCULATION RESULTS

Fig. 1 shows the atomistic structure of crystalline γ -Al₂O₃(110)/ β -Ga₂O₃(010) and *am*-Al₂O₃/ β -Ga₂O₃($\bar{2}01$) interface. Fig. 3 shows that the oxygen layers of the crystal structure are capable of forming stack structures with low lattice mismatched (2.2%). The purple circle is an overlapping

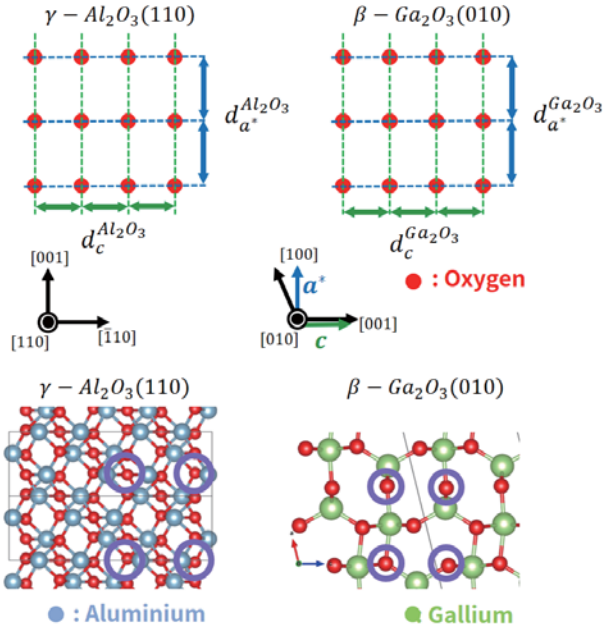


Figure 3 : Schematic drawings of oxygen atoms on $\gamma - Al_2O_3(110)$ and $\beta - Ga_2O_3(010)$. In the schematic diagram, the red circles indicate the positions of the oxygen atoms when viewed from each interface direction. This corresponds to the position of the oxygen atom indicated by the purple circle in the bottom pictures which is representing crystal structures of both material.

pair in the generated interface model. Fig 1(a), two interfaces in the crystalline structure are not perfectly matched, so that the combined interface can be obtained through structural optimization. As shown in Fig. 3, the model is created by matching the positions of oxygen atoms. The interfaces are optimized by DFT-MD simulations.

Fig. 4 depicts the electronic band structure of the $\gamma - Al_2O_3(110)/\beta - Ga_2O_3(010)$ interface structure and projector-density of state (PDOS) for each type of atoms. The structure of the lowest conduction band is similar to $\beta - Ga_2O_3$. 4.64eV indirect bandgap (Γ to $A - Z$) path is observed.

Fig. 5 shows a schematic diagram of the variations of the valence band maximum(VBM) and conduction band minimum(CBM) levels along the direction perpendicular to the interface. In Fig. 5(a), $\gamma - Al_2O_3(110)/\beta - Ga_2O_3(010)$ interface, the band offset of the conduction band side, ΔE_C , is 2.24eV and the one of the valence band side, ΔE_V , is 1.13eV. Fig. 5(b) shows the band offset result of $am - Al_2O_3/\beta - Ga_2O_3(\bar{2}01)$ interface (see Fig. 1 (c)). The band offset of the conduction band side, ΔE_C , is 1.83eV and the one of the valence band side, ΔE_V , is 1.07eV. The results of the DFT calculations show that the offset is slightly larger than the experimental values. Calculation results can provide some useful material parameters for the TCAD simulation.

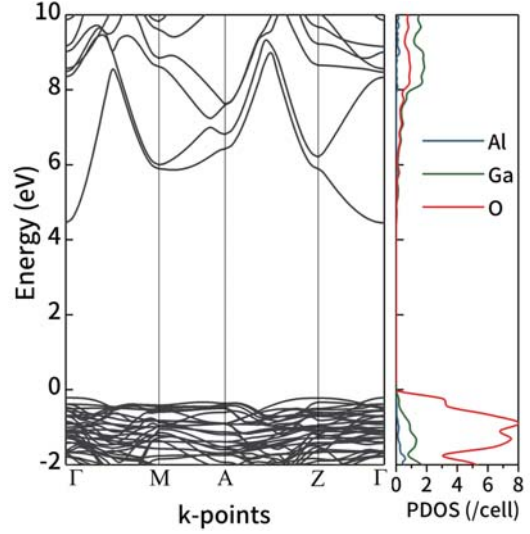


Figure 4 : Electronic band structure and projector density of states(PDOS) of the $\gamma - Al_2O_3(110)/\beta - Ga_2O_3(010)$ crystalline interface. An indirect band path is Γ to $A - Z$ and corresponding gap is 4.64eV. In valence bands, oxygen atoms occupy the most PDOS of the interface structure, and in the conduction band, gallium atoms have the largest PDOS in low bands. (lower than 10eV)

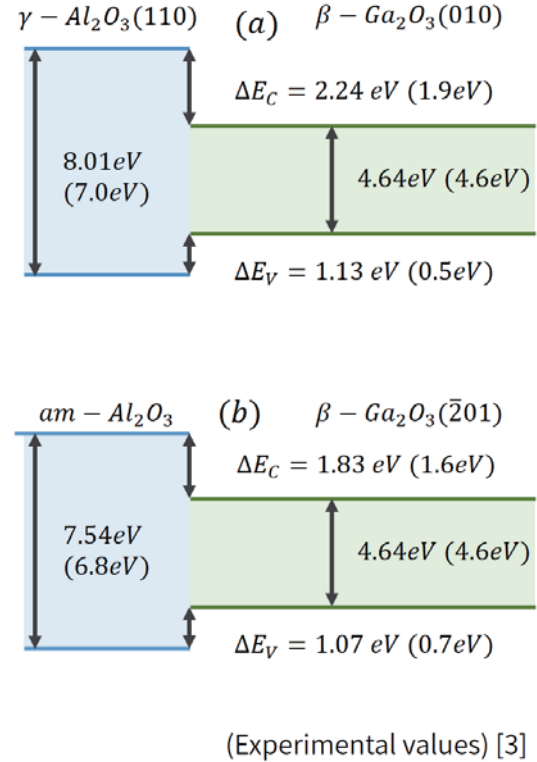


Figure 5 : VBM and CBM levels along the direction perpendicular to the interface plane. (a) band offset result of $\gamma - Al_2O_3(110)/\beta - Ga_2O_3(010)$ interface and (b) band offset result of $am - Al_2O_3/\beta - Ga_2O_3(\bar{2}01)$ interface.

IV. CONCLUSION

The atomistic models of $Al_2O_3/\beta-Ga_2O_3$ are presented. By the DFT based structural optimization, we obtain a structure estimated to be the stable structure. The electronic structure calculation shows the PDOS, in-plane band structure, position dependent electronic structure of the interfaces, and in-plane band offset characteristics. According to calculation results, it is expected that $Al_2O_3/\beta-Ga_2O_3$ interfaces are suitable dielectric-semiconductor interface for $\beta-Ga_2O_3$ based electronic devices.

REFERENCES

- [1] S. Stepanov, V. Nikolaev, V. Bougrov, and A. Romanov, "Gallium oxide: properties and applica a review," *Reviews on Advanced Materials Science*, vol. 44, pp. 63–86, 2016.
- [2] M. Higashiwaki, A. Kuramata, H. Murakami, and Y. Kumagai, "State-of-the-art technologies of gallium oxide power devices," *Journal of Physics D: Applied Physics*, vol. 50, no. 33, p. 333002, 2017.
- [3] S. Pearton, J. Yang, P. H. Cary IV, F. Ren, J. Kim, M. J. Tadjer, and M. A. Mastro, "A review of Ga_2O_3 materials, processing, and devices," *Applied Physics Reviews*, vol. 5, no. 1, p. 011301, 2018.
- [4] T. Kamimura, D. Krishnamurthy, A. Kuramata, S. Yamakoshi, and M. Higashiwaki, "Epitaxially grown crystalline Al_2O_3 interlayer on $\beta-Ga_2O_3$ (010) and its suppressed interface state density," *Japanese Journal of Applied Physics*, vol. 55, no. 12, p. 1202B5, 2016.
- [5] M. Hattori, T. Oshima, R. Wakabayashi, K. Yoshimatsu, K. Sasaki, T. Masui, A. Kuramata, S. Yamakoshi, K. Horiba, H. Kumigashira *et al.*, "Epitaxial growth and electric properties of $\gamma-Al_2O_3$ (110) films on $\beta-Ga_2O_3$ (010) substrates," *Japanese Journal of Applied Physics*, vol. 55, no. 12, p. 1202B6, 2016.
- [6] G. Kresse and J. Furthmüller, "Efficiency of ab-initio total energy calculations for metals and semiconductors using a plane-wave basis set," *Computational Materials Science*, vol. 6, no. 1, pp. 15–50, 1996.
- [7] J. P. Perdew, K. Burke, and M. Ernzerhof, "Generalized gradient approximation made simple," *Physical Review Letters*, vol. 77, no. 18, p. 3865, 1996.
- [8] D. Koller, F. Tran, and P. Blaha, "Merits and limits of the modified Becke-Johnson exchange potential," *Physical Review B*, vol. 83, no. 19, p. 195134, 2011.
- [9] J. P. Perdew, W. Yang, K. Burke, Z. Yang, E. K. Gross, M. Scheffler, G. E. Scuseria, T. M. Henderson, I. Y. Zhang, A. Ruzsinszky *et al.*, "Understanding band gaps of solids in generalized Kohn–Sham theory," *Proceedings of the National Academy of Sciences*, vol. 114, no. 11, pp. 2801–2806, 2017.
- [10] D. Koller, F. Tran, and P. Blaha, "Improving the modified Becke-Johnson exchange potential," *Physical Review B*, vol. 85, no. 15, p. 155109, 2012.
- [11] H. Jiang, "Band gaps from the Tran-Blaha modified Becke-Johnson approach: A systematic investigation," *The Journal of chemical physics*, vol. 138, no. 13, p. 134115, 2013.
- [12] M. Yazdanmehr, S. J. Asadabadi, A. Nourmohammadi, M. Ghasemzadeh, and M. Rezvani, "Electronic structure and bandgap of $\gamma-Al_2O_3$ compound using mBJ exchange potential," *Nanoscale Research Letters*, vol. 7, no. 1, p. 488, 2012.
- [13] G. Rehman, M. Shafiq, R. Ahmad, S. Jalali-Asadabadi, M. Maqbool, I. Khan, H. Rahnamaye-Aliabad, I. Ahmad *et al.*, "Electronic Band Structures of the Highly Desirable III–V Semiconductors: TB-mBJ DFT Studies," *Journal of Electronic Materials*, vol. 45, no. 7, pp. 3314–3323, 2016.
- [14] B. Narayanan, A. C. van Duin, B. B. Kappes, I. E. Reimanis, and C. V. Ciobanu, "A reactive force field for lithium–aluminum silicates with applications to eucryptite phases," *Modelling and Simulation in Materials Science and Engineering*, vol. 20, no. 1, p. 015002, 2011.
- [15] S. Davis and G. Gutiérrez, "Structural, elastic, vibrational and electronic properties of amorphous Al_2O_3 from ab initio calculations," *Journal of Physics: Condensed Matter*, vol. 23, no. 49, p. 495401, 2011.